

Effects of zinc and strontium substitution in tricalcium phosphate on osteoclast differentiation and resorption

Cite this: *Biomater. Sci.*, 2013, **1**, 74

Mangal Roy, Gary A. Fielding, Amit Bandyopadhyay and Susmita Bose*

Bone replacement materials must be able to regulate both osteoblastic synthesis of new bone and osteoclastic resorption process in order to maintain the balance of bone remodeling. Osteoclasts generate from differentiation of mononuclear cells. In the present study, we have studied osteoclast-like-cell responses (differentiation from mononuclear cells and resorption) to beta tricalcium phosphate (β -TCP) doped with zinc (Zn) and strontium (Sr). Osteoclast-like-cell differentiation and resorption was studied *in vitro* using an osteoclast-like-cell precursor RAW 264.7 cell, supplemented with receptor activator of nuclear factor $\kappa\beta$ ligand (RANKL). Morphological and immunohistochemical analysis confirmed successful differentiation of the osteoclast-like-cells on the doped and undoped β -TCP substrates after 8 days of culture. Cells on the substrate surface expressed specific osteoclast markers such as; actin rings, multiple nuclei, tartrate-resistant acid phosphatase (TRAP) synthesis, and vitronectin receptors. However, quantitative TRAP assay indicated the inhibitory effect of Zn on osteoclast differentiation. Although, Zn doped β -TCP restricted osteoclast-like-cell differentiation, the samples were resorbed much faster. An increased resorption pit volume was noticed on Zn doped β -TCP samples after 28 days of culture compared to pure and Sr doped β -TCP. In this work, we demonstrated that β -TCP bone substitute materials can be successfully resorbed by osteoclast-like-cells, where both osteoclast-like-cell differentiation and resorption were modulated by Zn and/or Sr doping—a much needed property for successful bone remodeling.

Received 21st March 2012,
Accepted 16th July 2012

DOI: 10.1039/c2bm00012a

www.rsc.org/biomaterialsscience

1. Introduction

Synthetic resorbable biomaterials are in ever increasing use for repairing or substituting damaged bones. The ideal material for this purpose should be osteoconductive with mechanical and resorbable properties matching that of bone. For resorbable bone substitute applications, where the implant dissolves while the host tissue replaces it, calcium phosphate (CaP) ceramics are widely used.^{1,2} Biodegradable CaPs, especially β -TCP, are extensively studied for reconstructive bone surgery due to its chemical similarity to bone.^{3–6} In biological systems, β -TCP dissolves by both chemical dissolution and osteoclastic resorption process, and prepares the surface for recruitment of osteoblast cells.⁷ On these diminished surfaces, new bone is formed by osteoblast cells and the bone remodeling process is initiated.

Bone remodels throughout life in a continuous process of osteoclastic resorption and osteoblastic synthesis of new bone. A shift in the equilibrium of this process can lead to osteoporosis, characterized by loss of bone density, or osteopetrosis

characterized by dysfunction of osteoclasts in resorbing bone.^{8,9} Therefore, resorbable bone replacement materials must be able to regulate both osteoblast and osteoclast functions in order to keep the dynamics of bone remodeling. The resorbable materials are expected to facilitate the bone remodeling process and are dissolved in due course. However, the resorption rate has to match with the patient's ability to form new bone, which depends on age, activity and the health condition of the patient.² Thus, the ability to regulate resorption properties is an added advantage for bone replacement materials.

Including certain metal dopants, which are naturally found in bone and known to contribute in the bone development process, is an attractive method to control the mechanical and biological properties of bone replacement materials.^{10,11} Our previous studies on SrO and MgO incorporated β -TCP have shown an enhanced *in vitro* osteoblast cell attachment, growth and improved *in vivo* biocompatibility.¹² We have also reported that osteoblast activity in TCP ceramics can be significantly enhanced by MgO doping.¹³ The advantageous effects of Sr in the bone turnover and treatment of osteoporosis has long been known.^{14,15} Even at 1.0 wt%, Sr doping in hydroxyapatite (HA) was found to increase osteoblast proliferation. Another trace element, zinc (Zn) is known to play a key role in significant functions in biological systems such as metalloenzymes,

W. M. Keck Biomedical Materials Research Laboratory School of Mechanical and Materials Engineering Washington State University, Pullman, WA 99164, USA.
E-mail: sbose@wsu.edu; Fax: +509-335-4662; Tel: +509-335-7461

including those involved in DNA and RNA replication and protein synthesis.^{16–18} Moreover, Zn deficiency is reported to reduce bone density and ductility, which increases the chance of bone fracture.¹⁹ Zn has also been reported to have an inhibiting factor for osteoclast differentiation, however, controversy exists in the published literature.^{16,17,19–21} Holloway *et al.* have shown that Zn increases the multinucleated TRAP positive cell number while inhibiting resorption over 24 h in co-cultures of osteoblasts and osteoclasts.²⁰ On the contrary, Yamada *et al.* reported a composition dependent increase in osteoclast apoptosis in Zn doped TCP samples.¹⁶ In a more recent study, it has been shown that Zn levels inside resorption lacuna could not influence the osteoclast activity in Zn-TCP samples.²¹ Therefore, it is worthwhile to understand the role of Zn in osteoclast differentiation.

The objective of the present study is to understand the role of Zn and Sr substitution in β -TCP towards controlling differentiation of mononuclear cells into osteoclast-like-cells and its resorptive activity. The influence of Zn and Sr doping on osteoclastogenesis was studied *in vitro* using an osteoclast-like-cell precursor cell RAW 264.7 supplemented with RANKL. Formation of osteoclast-like-cells was confirmed by cellular morphology, actin ring formation and multiple nuclei. In addition, the osteoclast-like-cell activity was studied by resorption lacunae formation.

2. Materials and methods

2.1 Materials processing

β -Tricalcium phosphate nanopowder (β -TCP) was obtained from Berkeley Advanced Biomaterials Inc. (Berkeley, CA, USA) with an average particle size of 550 nm. High purity strontium oxide (SrO, 99.9% purity) was purchased from Aldrich (MO, USA) and zinc oxide (ZnO, 99.998%) was procured from Alfa Aesar (MA, USA). Table 1 shows the four compositions of TCP used for this study. Samples were prepared by mixing 50 g β -TCP powder and appropriate amounts of dopants in 250 mL polypropylene Nalgene bottles containing 75 mL of anhydrous ethanol and 100 g zirconia milling media. The mixtures were then milled for 6 h at 70 rpm to minimize the formation of agglomerates, and increase homogeneity. After milling, the powder was dried in an oven at 60 °C for 72 h and pressed into disc shapes (12 mm diameter and 2.5 mm thickness) using a uniaxial press at 145 MPa. Green compacts were then cold

isostatically pressed at 414 MPa for 5 min and sintered at 1250 °C for 2 h in a muffle furnace. The apparent density of each composition was determined by the Archimedes' method and reported as relative density after normalizing to the theoretical density of β -TCP, *i.e.*, 3.07 g cm^{−3}. Average grain size was determined from FESEM images *via* a linear intercept method using the equation $G = [L/N] C$, where G is the average grain size (μm), L is the test line length (cm), N is the number of intersections with grain boundaries along test line L ; and C is the conversion factor (μm/cm) of the picture on which the test lines were drawn as obtained from the scale bar. For each composition, 30 lines from 3 samples were used to calculate the grain size. The data is reported as mean ± standard deviation. A Siemens D500 Krystalloflex X-ray diffractometer using Cu K α radiation at 35 kV and 30 mA at room temperature was used to determine different phases with a Ni-filter over the 2 θ range between 20° and 45°, at a step size of 0.02° and a count time of 0.5 s per step.

2.2 Osteoclast cell culture

The human monocyte-like cell line RAW 264.7 (ATCC, USA) was cultured in DMEM media (ATCC, USA) supplemented with 10 vol.% fetal bovine serum (FBS, Sigma, Germany) and 1 vol.% penicillin-streptomycin (Invitrogen, Germany) at 37 °C in an atmosphere of 5% CO₂. Cells were grown for 3 days in 25 cm² culture flasks (Nunc, Denmark). After reaching confluence, the cells were scraped off from the culture flask using a cell scraper. β -TCP disks were autoclaved at 121 °C for 20 min and then RAW 264.7 cells were seeded at a concentration of 10⁵ cells per ml and incubated at 37 °C in an atmosphere of 5% CO₂. At day 1, 50 ng ml^{−1} RANKL (Biologen, CA, USA) was added to the culture media. After this period, cell media, containing 50 ng ml^{−1}, was changed every 2 days for the duration of the experiment. For the control, TCP, Zn-TCP, Sr-TCP and Zn/Sr-TCP disks were also incubated with RAW 264.7 cells at 37 °C in an atmosphere of 5% CO₂; however, the media was not supplemented with RANKL.

2.3 Osteoclast cell morphology

The morphology of the cells was assessed by field emission scanning electron microscope (FESEM, FEI 200F, FEI Inc., OR, USA). Samples were removed from culture after 3, 5 and 8 days of incubation and were rinsed with 0.1 M phosphate-buffered saline (PBS). Samples were subsequently fixed with 2% paraformaldehyde–2% glutaraldehyde in 0.1 M cacodylate buffer overnight at 4 °C. Following a rinse in 0.1 M cacodylate buffer, each sample was post-fixed in 2% osmium tetroxide (OsO₄) for 2 h at room temperature. Fixed samples were then dehydrated in an ethanol series (30%, 50%, 70%, 95% and 100% three times), followed by hexamethyl-disililane (HMDS) drying. Dried samples were gold coated and observed under FESEM for cell morphologies.²²

2.4 TRAP activity

Tartrate resistant acid phosphatase (TRAP) activity, a characteristic of osteoclasts, was measured according to the

Table 1 Relative density and grain size of undoped and doped samples

Sample	Composition	Relative density (%)	Grain size (μm)
TCP	β -TCP	96.17 ± 0.89	4.09 ± 0.69
Zn-TCP	β -TCP + 0.25 wt% Zn	98.07 ± 0.52	3.05 ± 0.33
Sr-TCP	β -TCP + 1.0 wt% Sr	95.02 ± 1.39	4.86 ± 0.84
Zn/Sr-TCP	β -TCP + 1.0 wt% Sr + 0.25 wt% Zn	95.31 ± 0.64	4.73 ± 0.71

protocol.^{23–25} After 5, 8 and 14 days of culture, adherent osteoclast-like-cells were lysed in 1 M NaCl with 0.2% Triton X-100. The lysate were incubated with 50 mL of 5 mM *p*-nitrophenyl phosphate (Sigma, USA) in 25 mM Na acetate–20 mM Na tartrate, pH 4.8 at 37 °C for 30 min. The reaction was stopped by adding 0.5 M NaOH. 100 µL of the resulting supernatant was transferred into a 96-well plate, and read by a plate reader at 405 nm. The data were reported as mean ± standard deviation. The Student's "t" test was used to determine the statistical significance.

2.5 Immunofluorescence and confocal laser-microscopy

After specific culture days, the osteoclast-like-cells were fixed in 3.7% paraformaldehyde-phosphate buffered solution, pH 7.4 and at room temperature for 10 min. After washing with PBS 3 times (5 min each), the cells were permeabilized with 0.1% Triton X-100 (in PBS) for 4 min at room temperature. Samples were then washed with PBS and incubated in a TBST-BSA (Tris-buffered saline with 1% bovine serum albumin, 250 mM NaCl, pH 8.3) blocking solution for 1 h at room temperature. Actin staining was done by incubating the samples in rhodamine–phalloidin (Molecular Probes, Invitrogen), diluted in PBS 1 : 40 for 30 min in the dark. Samples were then rinsed in PBS and incubated in the primary antibody (mouse anti-vitronectin, Abcam), with 1 : 50 in TBST solution for 2 h and kept at 4 °C overnight. Samples were then washed with TBST-BSA for 10 min 3 times. The secondary antibody (Alex Fluor 488 anti-mouse) was diluted 1 : 100 in TBST and was used to incubate the cells for 1 h. After 2 × 5 min washing with TBST-BSA followed by 5 min washing with PBS, the samples² were then mounted on glass coverslips with Vectashield mounting medium (Vector Labs, Burlingame, CA) with 4',6-diamidino-2-phenylindole (DAPI) and kept at 4 °C for future imaging. The microscopic examinations were performed on a Zeiss 510 laser scanning microscope (LSM 510 META, Carl Zeiss MicroImaging, Inc., NY, USA).

2.6 Resorption pit assay

Osteoclast-like-cells were removed from the sample surface after 14, 21 and 28 days of culture. Samples were ultrasonicated in 1 M NaCl solution with 0.2% Triton X-100 to remove the osteoclast-like-cells and then washed with PBS.²⁵ After gold coating, the samples were observed in FESEM for resorption lacuna. To ensure that the surface degradation of the TCP ceramics are related to osteoclast-like-cellular activity and not related to chemical degradation, TCP disks were kept in culture media and cells; however, RANKL was not added in the media and were used as controls.

2.7 Ca²⁺ concentration in the media

Ca²⁺, Sr²⁺, Zn²⁺ ion content in the culture media was measured using a Shimadzu AA-6800 atomic absorption spectrophotometer (Shimadzu, Kyoto, Japan). Culture media was diluted to 1 : 50 using deionized water and 1% strontium chloride. For the measurement of Sr²⁺ and Zn²⁺, culture media was diluted

to 1 : 100 in deionized water. The data were reported as mean ± standard deviation (*n* = 9).

3. Results

3.1 Physico-chemical properties

X-ray diffraction (XRD) patterns of sintered TCP samples with and without dopants are shown in Fig. 1. The majority of the peaks resemble the β-TCP (JCPDS #09–169) phase. Few peaks related to the α-TCP (JCPDS #09–0348) phase were also identified in the XRD pattern of undoped TCP samples indicating phase transition during sintering. However, α-TCP peaks were not detected in Zn-TCP and Zn/Sr-TCP. A very weak peak of α-TCP was detected for Sr-TCP samples. The relative density of TCP, Zn-TCP, Sr-TCP and Zn/Sr-TCP were found to be 96.17 ± 0.89%, 98.07 ± 0.52%, 95.02 ± 1.39%, and 95.31 ± 0.64%, respectively.

The influence of dopants on the grain size of sintered TCP compacts are shown in Fig. 2. Addition of Zn reduced the grain size of the Zn-TCP samples to 3.05 ± 0.33 µm compared to that of 4.09 ± 0.69 µm of TCP samples. The grain size in Sr-TCP increased to 4.86 ± 0.84 µm, a statistically significant increase from that of pure TCP. Formation of some glassy phase was also observed for Sr-TCP samples. The binary Zn/Sr doped TCP samples had 4.73 ± 0.71 µm sized grains. The grain size distribution was narrow and uniform for TCP and Zn-TCP samples. However, a wide grain size distribution was noticed in Sr-TCP and Zn/Sr-TCP samples. Table 1 summarizes the physical properties of the doped and undoped TCP samples.

3.2 Osteoclast cell phenotype

The osteoclast-like-cell morphology and its interaction with β-TCP substrates was analyzed using FESEM. Fig. 3 shows the RAW 264.7 cell morphology on TCP, Zn-TCP, Sr-TCP, and Zn/Sr-TCP samples after 5 days of culture. Spontaneous

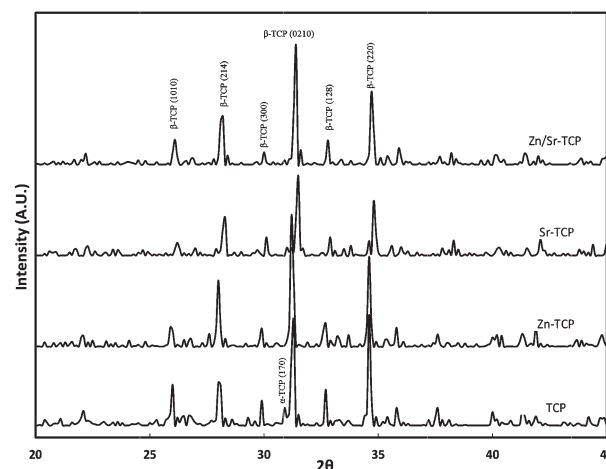


Fig. 1 X-ray powder diffraction patterns of TCP, Zn-TCP, Sr-TCP, and Zn/Sr-TCP sintered at 1250 °C.

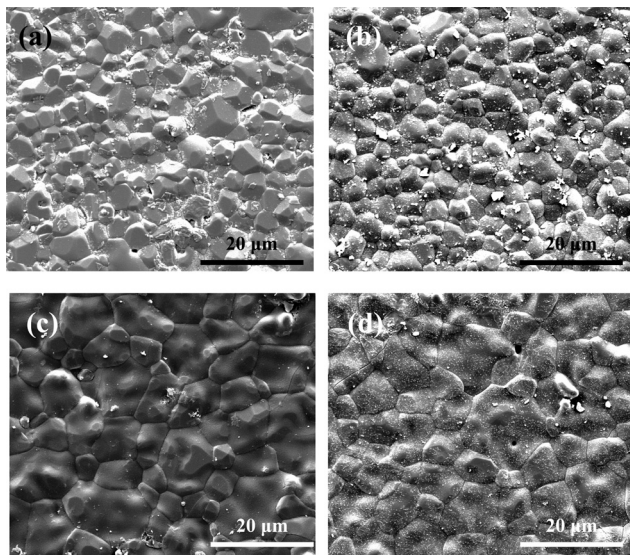


Fig. 2 Influence of dopant addition on grain size of sintered tricalcium phosphate. (a) – pure TCP with average grain size $4.09 \pm 0.69 \mu\text{m}$, (b) – Zn-TCP with average grain size $3.05 \pm 0.33 \mu\text{m}$, (c) – Sr-TCP with average grain size $4.86 \pm 0.84 \mu\text{m}$ and (d) – Zn/Sr-TCP with average grain size $4.73 \pm 0.71 \mu\text{m}$.

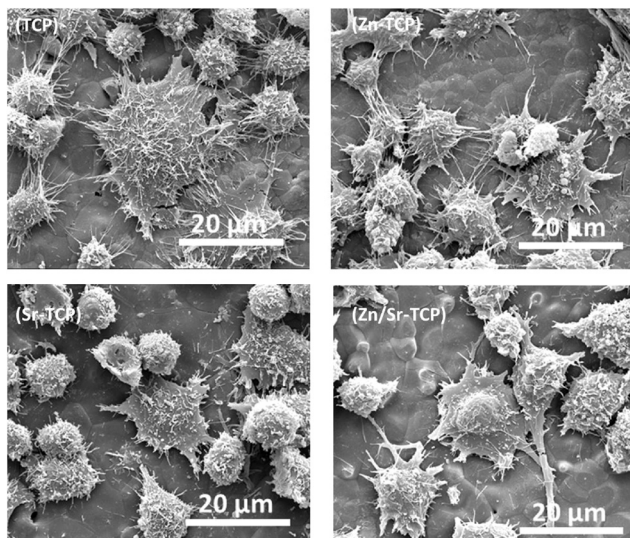


Fig. 3 FE-SEM micrographs illustrating the RAW 264.7 cell morphologies after 5 days of culture with RANKL.

adhesion of cells was noticed on all of the TCP substrates with extensive cellular micro-extensions. Morphologically, these cells resembled RAW 264.7 monocytes with few of them initiating differentiation to osteoclast-like-cells. After 8 days of culture, the cellular morphology on TCP substrates is shown in Fig. 4. The cells on all of the TCP substrates grew in size from day 5 and had a completely different morphology than the monocytes. Round and giant cells with well-organized cell membranes, characteristics of osteoclast, was noticed. The characteristic “blebs” can be noticed on the cell surfaces.

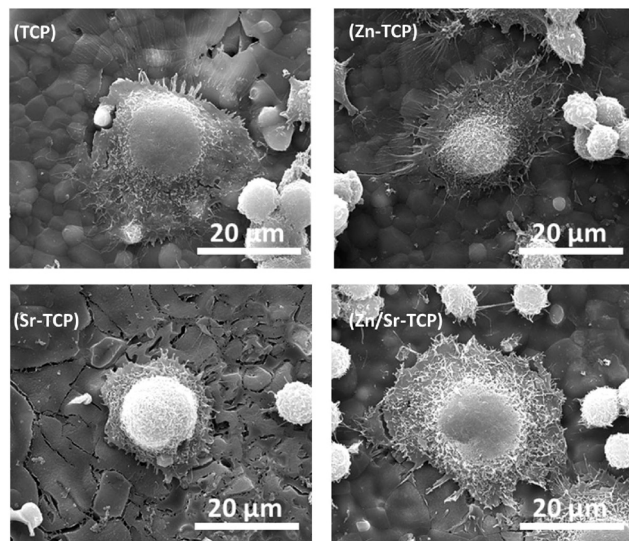


Fig. 4 FE-SEM micrographs illustrating osteoclast-like-cell morphologies after 8 days of culture with RANKL.

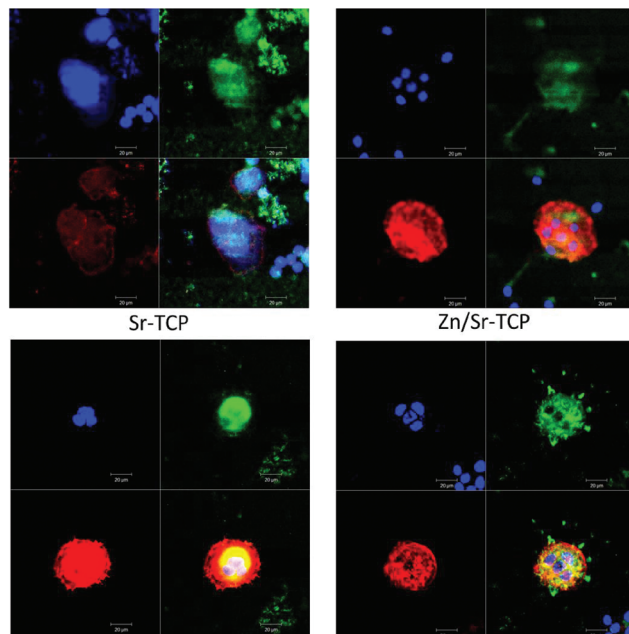


Fig. 5 Fluorescence microscopy showing actin rings (red), nuclei (blue), and vitronectin receptor $\alpha_v\beta_3$ integrin (green) after 8 days of culture.

To ensure that the giant cells are osteoclast-like-cells, we tested them for specific markers such as actin rings, vitronectin receptors and multinuclearity after 8 and 14 days of culture. Fig. 5 shows the fluorescence microscope images of RAW 264.7 cells cultured on doped or undoped TCP samples for 8 days. Cultured cells were multinuclear with prominent actin rings at the periphery. The $\alpha_v\beta_3$ integrin, a vitronectin receptor protein, was highly expressed in the cell's plasma membrane and cytoplasm. Significant differences were not found in phenotypic expressions of the osteoclast-like-cells cultured on three doped TCP samples. Fig. 6 shows confocal

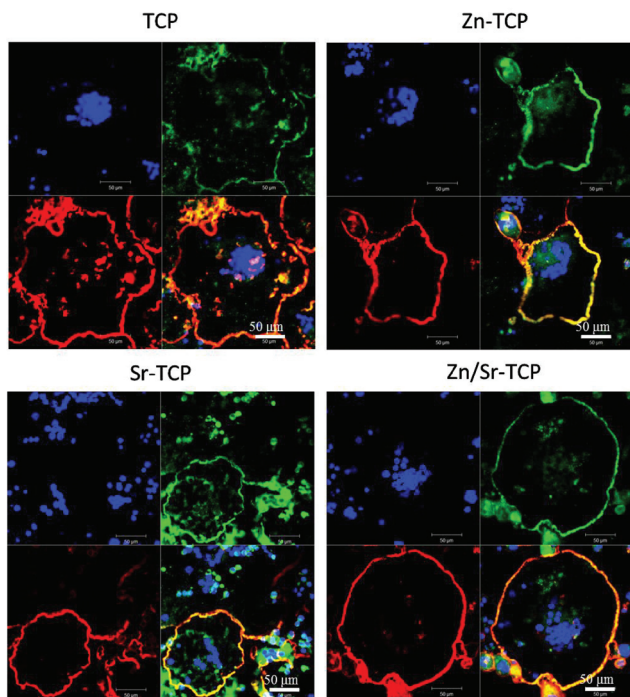


Fig. 6 Fluorescence microscopy images of cells cultured for 14 days. The red represents the actin cytoskeleton, green indicates vitronectin receptor $\alpha_v\beta_3$ integrin and blue represents the nucleolus.

micrographs of the osteoclast-like-cells on different TCP substrates after 14 days of culture. Cells were found to be multi-nuclear with continuous actin rings on all three samples. Podosomes were noticed at the periphery of the cells along with vitronectin receptor $\alpha_v\beta_3$.

3.3 TRAP assay

Tartrate-resistant acid phosphatase (TRAP) is highly expressed by osteoclasts. For this reason, TRAP expression was evaluated as a marker for osteoclast phenotype. TRAP synthesized by osteoclast-like-cells are shown in Fig. 7 as a function of culture days and chemical compositions. An increase in TRAP concentration was evident over the duration of the experiment. Negligible TRAP activity was detected after culturing RAW 264.7 cells on doped and undoped TCP samples for 5 days. At day 8, synthesis of TRAP by osteoclast-like-cells was significantly higher on pure TCP substrates. Addition of dopants reduced the TRAP activity; however, the statistical significance was only reached for Zn-TCP samples. After 14 days of culture, TRAP activity increased in all TCP samples although the reduction in Zn-TCP samples was noticed.

3.4 Surface resorption

Resorptive activity of the osteoclast-like-cells was determined by removing cells and observing changes in surface features. Fig. 8 shows the difference in surface morphology between the doped and undoped TCP samples along with their control samples after 14 days of culture. Control samples did not show any chemical degradation of the surfaces. No obvious

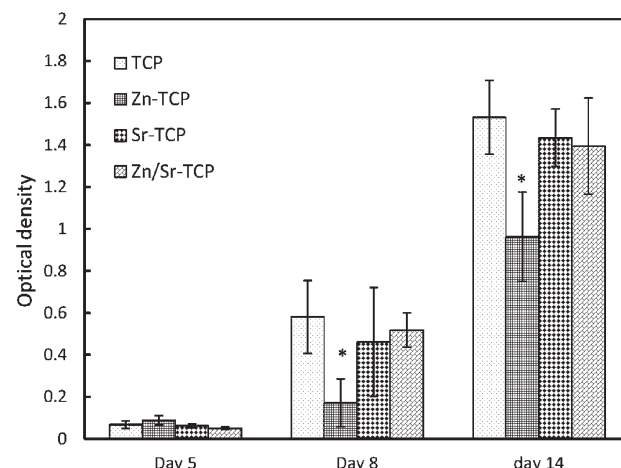


Fig. 7 TRAP assay as a function of culture days. (*Statistical difference $p < 0.05$, $n = 3$).

resorption lacuna was noticed on any of the four TCP substrates. However, round impressions, resembling the size and shape of osteoclast-like-cells, were found on the sample surfaces. Resorption lacunae on the sample surfaces after 21 days of culture are shown in Fig. 9. No such resorption lacunae were noticed on the control samples. Instead, some small etch pits were found, which was primarily due to chemical degradation of the samples. Compared to day 14, prominent resorption pits were found after 21 days. Resorption pits on TCP surfaces were mostly surface phenomenon where pits with bulk degradation were noticed in Zn-TCP, Sr-TCP and Zn/Sr-TCP.

At day 28, a significant increase in depth of the resorption pits was noticed in TCP and Zn-TCP samples, as shown in Fig. 10. Some random degradation sites (degradation of the resurface due to osteoclast-like-cells are generally confined to a particular location and large in size) were noticed on TCP control samples after 28 days indicating chemical degradation that was not related to osteoclast-like-cell degradation.

3.5 Ionic concentration in the media

Osteoclast-like-cellular resorption behavior was quantified by measuring Ca^{2+} concentration in the culture media. Fig. 11a-d shows Ca^{2+} release from TCP substrates as a function of culture days and composition. To distinguish the chemical degradation from osteoclast-like-cellular resorption, control disk samples of similar composition was also cultured with RANKL deprived media. The resorption behavior was similar for all four compositions. However, Sr-TCP control samples showed the highest initial dissolution compared to all other samples. Zn-TCP and Zn/Sr-TCP samples had the lowest concentration of Ca^{2+} in the culture media for all the culture days. Interestingly, Ca^{2+} concentration did not increase in the culture media for samples with osteoclasts. The only statistically significant difference was noticed in Zn-TCP after 28 days of culture. Sr and Zn ionic concentrations in the media are shown in Fig. 12. There were no statistical difference in Sr and

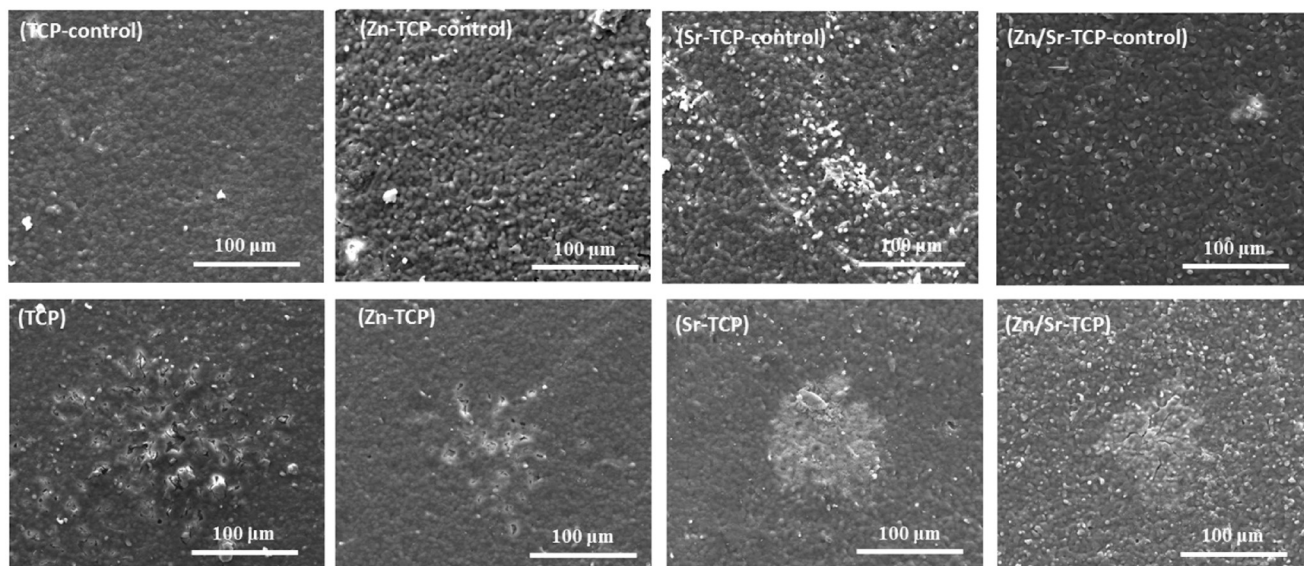


Fig. 8 Surface morphology of doped and undoped TCP samples after culturing with RAW 264.7 cells at day 14. Round impressions of osteoclast-like-cells were visible on the sample surfaces.

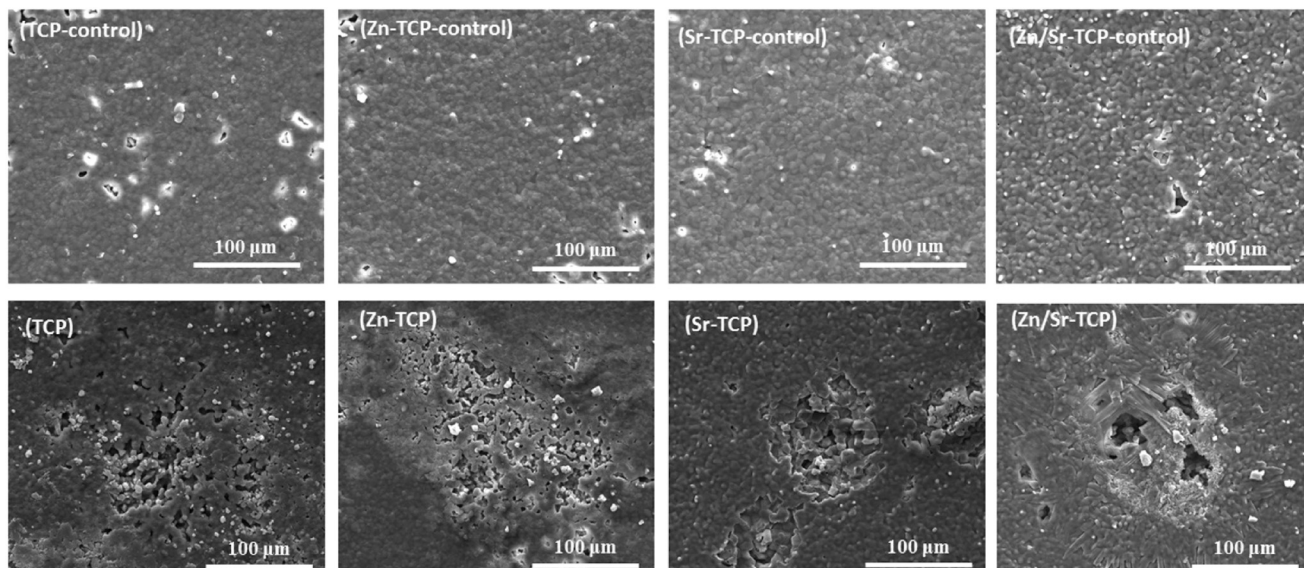


Fig. 9 Surface morphology of doped and undoped TCP samples after culturing with RAW 264.7 cells at day 21. Prominent resorption lacunae were noticed on Sr-TCP and Zn/Sr-TCP samples.

Zn ion concentrations between the control samples and the RANKL treated samples at any culture point. Cumulatively less than 100 parts per billion (ppb) Zn ions was found in the culture media after 2 days. In comparison, a much higher Sr ion concentration was noticed in both Sr-TCP and Zn/Sr-TCP samples.

4. Discussion

In this study, the effects of Zn and Sr dopants in β -TCP on osteoclast-like-cell formation and its activity is demonstrated.

In our model system, transformation of the β -TCP to the α -TCP phase is retarded by Zn and Sr doping. Zn is known to increase the transformation temperature of β to α phase of TCP.^{26,27} Because of a smaller ionic radius, Ca^{2+} (0.99 Å) substitution by Zn^{2+} (0.74 Å) in β -TCP results in unit cell volume shrinkage and higher density. On the other hand, larger ionic sized Sr^{2+} (1.13 Å) substitution leads to unit cell volume expansion and lower density.²⁶ Because of a higher percentage of Sr compared to Zn, the net effect of Zn and Sr co-substitution is grain growth of β -TCP.

To understand the role of Zn and/or Sr on osteoclast-like-cell differentiation, phenotypic expressions of osteoclasts are

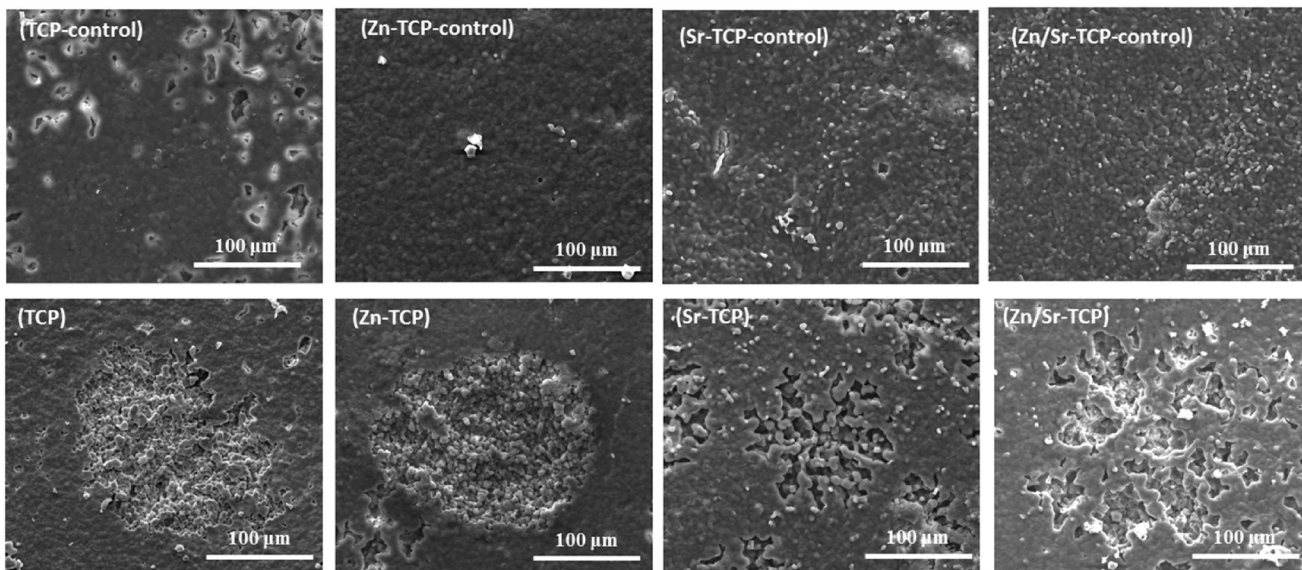


Fig. 10 Surface morphology of doped and undoped TCP samples after culturing with RAW 264.7 cells at day 28. Resorption lacunae were found on all the sample surfaces. Bulk degradation can be noticed in TCP and Zn-TCP substrates.

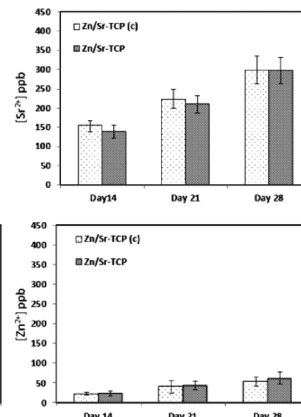
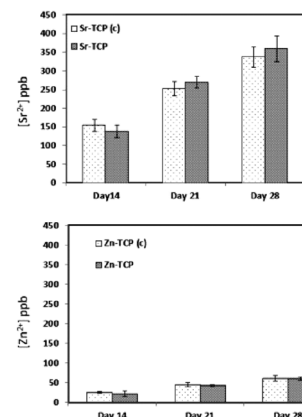
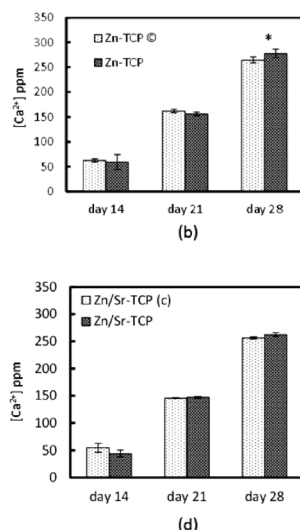
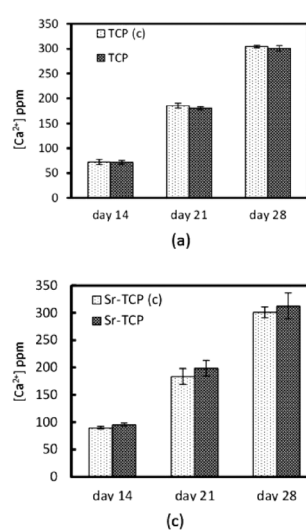


Fig. 11 Calcium concentration in the medium at different time points for TCP samples with and without osteoclast-like-cells. (*Statistical difference $p < 0.05$, $n = 9$).

studied on pure and doped β -TCP samples. During initial time period, monocytes use cellular microextensions, such as lamellipodia and filopodia to adhere to the substrate. The presence of these cellular features after 5 days of culture shows that the RAW 264.7 cells spontaneously adhere to all the β -TCP substrates. Morphological similarity of the cells attached to the undoped and doped β -TCP substrates indicate that the dopants have an insignificant effect on initial cell attachment. Morphological analysis also indicates that the RAW 264.7 monocytes have not completely differentiated to osteoclast-like-cells on any of the β -TCP substrates. The results are also confirmed by TRAP assay. The absence of significant

TRAP activity after 5 days of culture confirms that the cells are not osteoclast-like-cells.

Formation of osteoclast-like-cells is noticed after 8 days of culture on all β -TCP substrates. Cellular morphology indicates the cells to be osteoclast-like-cells with far reaching pseudopodia attached to the substrate surface. Immunohistochemical analysis also confirms the differentiation of RAW 264.7 cells to osteoclast-like-cells. It is well known that multinuclearity and formation of actin rings are the essential characteristic markers of osteoclasts.⁹ The presence of these markers indicates that pure and undoped β -TCP substrates allow osteoclast-like-cell differentiation. From single cell phenotypic expressions, osteoclast-like-cells appear to be successfully differentiated on all the β -TCP substrates without any inhibiting effects from the dopants. However, a quantitative study, determined through TRAP assay, shows the effects of Zn, Sr,

and binary doping on osteoclast-like-cell differentiation. Compared to day 5, a significantly higher TRAP activity at day 8 indicates that the cells have successfully differentiated to osteoclast-like-cells at day 8. The inhibitory effect of Zn in osteoclast-like-cell differentiation is evident in TRAP assay at day 8 and can be explained through different mechanisms. Studies have shown that Zn can significantly repress basal NF- κ B in osteoclast precursor cells *in vitro*.²⁸ Furthermore, it has been demonstrated that the presence of Zrt-Irt-like proteins (ZIP1), a ubiquitous plasma membrane zinc transporter and responsible for Zn uptake in osteoclasts, are overexpressed in the presence of Zn.¹⁷ This ZIP1 has a profound inhibitory effect on the differentiation of osteoclasts. ZIP1 also blocks the signaling pathway for NF- κ B, which is essential for osteoclast differentiation. It has also been reported that although Zn concentration does not significantly increase in the extracellular environment, it can lead to osteoclast apoptosis.¹⁶ In comparison, the presence of Sr in the Sr-TCP samples does not affect osteoclastogenesis. The ineffectiveness of Sr on the osteoclastogenesis is also supported by the work of Rousselle *et al.* where it has been reported that up to 10 ppm Sr²⁺ in the culture media does not alter osteoclast size or number.²⁹ In the present work, a total of 400 ppb Sr ion is recorded, indicating that the soluble Sr ion has no effect on osteoclastogenesis. After 14 days of culture, the effect of Zn on osteoclast-like-cell activity is more pronounced. Sr doped β -TCP substrate also reduces the TRAP activity; however, it is not statistically significant. In Zn/Sr-TCP samples, the statistically insignificant difference in TRAP activity is primarily because of a relatively higher percentage of Sr than Zn.

Surface resorption of pure and doped TCP samples is monitored at 14, 21 and 28 days of culture in order to evaluate the resorative activity of osteoclast-like-cells. After 14 days of culture, formation of osteoclast-like-cell imprints on the sample surfaces indicates attachment and onset of osteoclast-like-cellular resorption. Immunohistochemical analysis after 14 days of culture also indicates that the differentiated osteoclast-like-cells are well attached to all the β -TCP substrates. In the sequence of osteoclast resorption, cells intimately attach to the surface using filamentous actin before initiating resorption.⁸ In addition, intramembranous integrin ($\alpha_v\beta_3$), a vitronectin receptor, plays a crucial role in cellular adherence.^{8,30} The presence of continuous actin rings and highly localized $\alpha_v\beta_3$ integrin indicates that the osteoclast-like-cells are strongly attached to the substrate surface and initiate resorption.

Once attached, the osteoclast-like-cells start resorbing bone by forming a tight seal to the surface, known as the "sealing zone".⁸ Under this sealing zone microenvironment, the pH can reach as low as 4.5 and degrade the mineral constituents of bone.⁸ Along with the environment, degradation of TCP samples is also dependent on phase purity, density, grain size, and the presence of impurities and amorphous phases.³¹ Formation of a glassy phase on the surface of Sr-TCP samples results in a higher initial resorption. An increase in Ca²⁺ concentration in the culture media indicates that the Sr-TCP samples have a higher chemical solubility than pure TCP

samples. It has been reported that Sr substitution in β -TCP results in lower crystallinity and increased dissolution.^{26,32} In contrast, Zn-TCP samples show higher stability in physiological conditions.^{7,26} Incorporation of Zn in β -TCP also helps in retarding the β -TCP \rightarrow α -TCP phase transition. As β -TCP has lower solubility than α -TCP, Zn-TCP samples show lower Ca²⁺ release in the culture media.

Zn-TCP and Zn/Sr-TCP samples having higher crystallinity and relatively stable β -TCP phase do not show abrupt early resorption. The resorption lacunae on these samples have slightly increased in diameter on day 21 but show a significant increase in depth. After 28 days, the resorption behavior has completely altered for pure and doped TCP samples. With a grain size of 4.09 ± 0.69 μ m, pure TCP samples have readily degraded at day 28 compared to day 21. The Zn-TCP samples also shows an increase in resorption, which can possibly be attributed to its smaller grain size (3.05 ± 0.33 μ m). In a recent article, increased osteoclast-like-cellular resorption of hydroxyapatite (similar bone substitute material) due to a decrease in grain size is reported.³¹ The increase in depth of resorption lacunae on Zn-TCP samples indicates that grain size plays an important role in osteoclast-like-cellular resorption kinetics. The statistically significant increase in Ca²⁺ release indicates that the Zn-TCP samples are significantly resorbed by the osteoclast-like-cells. Although TRAP assay shows a reduction in osteoclast-like-cell differentiation due to the presence of Zn, an increase in Ca²⁺ concentration indicates small numbers of differentiated osteoclast-like-cells are highly active on these Zn-TCP samples. In comparison, resorption lacunae on Sr-TCP samples do not significantly increase in depth on day 28 compared to day 21. One possible reason could be the larger grains in Sr-TCP samples, which are not readily resorbed by osteoclast-like-cells. Similarly, Zn/Sr-TCP samples having a bigger grain size (4.73 ± 0.71 μ m) also show reduced resorption compared to TCP or Zn-TCP samples.

Here we show that in the presence of sufficient amounts of RANKL, osteoclastogenesis and its resorative activity can be controlled on TCP ceramics by Zn doping. Our findings show a way of controlling osteoclast-like-cell mediated resorption of TCP ceramics, based on chemistry. Under *in vivo* conditions, TCP degrades by chemical dissolution and osteoclastic resorption process. The present results can be combined with published literature of chemical dissolution to design a resorbable TCP bone substitutes with much more controlled degradation properties.

Conclusions

This study indicated chemistry dependent osteoclastogenesis on β -TCP substrates and its activity. Osteoclast precursor monocytes were spontaneously attached to all the substrate surfaces and differentiated to osteoclast-like-cells with the addition of RANKL. The presence of actin rings, multiple nuclei and positivity for vitronectin receptor $\alpha_v\beta_3$ integrin confirmed the cells to be osteoclast-like-cells. In the presence of

Zn, TRAP activity was reduced significantly in all the culture days. However, the presence of Zn did not affect the osteoclast-like-cellular resorption process. Smaller grain sized Zn-TCP samples showed deeper resorption lacunae formation compared to pure or other doped samples. The present results can be used to develop bone replacement materials which can modulate osteoclastogenesis and its resorption kinetics based on application site and patients individual requirements.

Acknowledgements

The authors acknowledge financial support from the National Institute of Health (N1H-RO1-EB-007351) for this research. Authors thank Dr Ted S Gross from the University of Washington for technical help and the Franceschi Microscopy and Imaging Center, Washington State University for their assistance in the immunohistochemical and FESEM analyses.

Notes and references

- 1 S. V. Dorozhkin and M. Epple, *Angew. Chem., Int. Ed.*, 2002, **41**, 3130–3146.
- 2 A. F. Schilling, W. Linhart, S. Filke, M. Gebauer, T. Schinke, J. M. Rueger and M. Amling, *Biomaterials*, 2004, **25**, 3963–3972.
- 3 A. Bandyopadhyay, S. Bernard, W. Xue and S. Bose, *J. Am. Ceram. Soc.*, 2006, **89**, 2675–2688.
- 4 N. Kondo, A. Ogose, K. Tokunaga, T. Ito, K. Arai, N. Kudo, H. Inoue, H. Irie and N. Endo, *Biomaterials*, 2005, **26**, 5600–5608.
- 5 T. Okuda, K. Ioku, I. Yonezawa, H. Minagi, G. Kawachi, Y. Gonda, H. Murayama, Y. Shibata, S. Minami, S. Kamihira, H. Kurosawa and T. Ikeda, *Biomaterials*, 2007, **28**, 2612–2621.
- 6 S. Tarafder, V. K. Balla, N. M. Davies, A. Bandyopadhyay and S. Bose, *J. Tissue Eng. Regenerative Med.*, 2012, DOI: 10.1002/term.555.
- 7 M. Kamitakahara, C. Ohtsuki and T. Miyazaki, *J. Biomater. Appl.*, 2008, **23**, 197–212.
- 8 S. L. Teitelbaum, *Science*, 2000, **289**, 1504–1508.
- 9 W. J. Boyle, W. S. Simonet and D. L. Lacey, *Nature*, 2003, **423**, 337–342.
- 10 L. Yang, S. Perez-Amodio, F. Y. F. Barrère-de Groot, V. Everts, C. A. van Blitterswijk and P. Habibovic, *Biomaterials*, 2010, **31**, 2976–2989.
- 11 A. Hoppe, N. S. Güldal and A. R. Boccaccini, *Biomaterials*, 2011, **32**, 2757–2774.
- 12 S. S. Banerjee, S. Tarafder, N. M. Davies, A. Bandyopadhyay and S. Bose, *Acta Biomater.*, 2010, **6**, 4167–4174.
- 13 W. Xue, K. Dahlquist, A. Banerjee, A. Bandyopadhyay and S. Bose, *J. Mater. Sci.: Mater. Med.*, 2008, **19**, 2669–2677.
- 14 P. J. Marie, *Osteoporosis Int.*, 2005, **16**, S7–S10.
- 15 C. Capuccini, P. Torricelli, F. Sima, E. Boanini, C. Ristoscu, B. Bracci, G. Socol, M. Fini, I. N. Mihailescu and A. Bigi, *Acta Biomater.*, 2008, **4**, 1885–1893.
- 16 Y. Yamada, A. Ito, H. Kojima, M. Sakane, S. Miyakawa, T. Uemura and R. Z. LeGeros, *J. Biomed. Mater. Res., Part A*, 2008, **84A**, 344–352.
- 17 M. A. Khadeer, S. N. Sahu, G. Bai, S. Abdulla and A. Gupta, *Bone*, 2005, **37**, 296–304.
- 18 S. Pina, S. I. Vieira, P. Rego, P. M. C. Torres, O. A. B. da Cruz e Silva, E. F. da Cruz e Silva and J. M. F. Ferreira, *Eur. Cell Mater.*, 2010, **20**, 162–177.
- 19 N. R. Calhoun, J. C. Smith Jr. and K. L. Becker, *Clin. Orthop. Relat. Res.*, 1974, 212–234.
- 20 W. R. Holloway, F. M. Collier, R. E. Herbst, J. M. Hodge and G. C. Nicholson, *Bone*, 1996, **19**, 137–142.
- 21 X. Li, K. Senda, A. Ito, Y. Sogo and A. Yamazaki, *Biomed. Mater.*, 2008, **3**, 045002.
- 22 M. Roy, A. Bandyopadhyay and S. Bose, *J. Am. Ceram. Soc.*, 2010, **93**, 3720–3725.
- 23 S. S. Banerjee, M. Roy and S. Bose, *Adv. Eng. Mater.*, 2011, **13**, B10–B17.
- 24 T. J. Webster, C. Ergun, R. H. Doremus, R. W. Siegel and R. Bizios, *Biomaterials*, 2001, **22**, 1327–1333.
- 25 S. Patntirapong, P. Habibovic and P. V. Hauschka, *Biomaterials*, 2009, **30**, 548–555.
- 26 S. Kannan, F. Goetz-Neunhoeffer, J. Neubauer and J. M. F. Ferreira, *J. Am. Ceram. Soc.*, 2011, **94**, 230–235.
- 27 A. Ito, H. Kawamura, S. Miyakawa, P. Layrolle, N. Kanzaki, G. Treboux, K. Onuma and S. Tsutsumi, *J. Biomed. Mater. Res.*, 2002, **60**, 224–231.
- 28 M. Yamaguchi and N. Weitzmann, *Mol. Cell. Biochem.*, 2011, **355**, 179–186.
- 29 A. V. Rousselle, D. Heymann, V. Demais, C. Charrier, N. Passuti and M. F. Baslé, *Histol. Histopathol.*, 2002, **17**, 1025–1032.
- 30 R. Detsch, H. Mayr and G. Ziegler, *Acta Biomater.*, 2008, **4**, 139–148.
- 31 R. Detsch, D. Hagmeyer, M. Neumann, S. Schaefer, A. Vortkamp, M. Wuelling, G. Ziegler and M. Epple, *Acta Biomater.*, 2010, **6**, 3223–3233.
- 32 H. B. Pan, Z. Y. Li, W. M. Lam, J. C. Wong, B. W. Darvell, K. D. K. Luk and W. W. Lu, *Acta Biomater.*, 2009, **5**, 1678–1685.